Fluorescence analysis allows to predict the oxidative capacity of humic quinones in dissolved organic matter: implication for pollutant degradation

Davide Palma, Edith Parlanti, Mahaut Sourzac, Olivier Voldoire, Aude Beauger, Mohamad Sleiman, Claire Richard

Environmental Chemistry Letters (2021) 19:1857–1863
https://doi.org/10.1007/s10311-020-01137-z

ORIGINAL PAPER

Fluorescence analysis allows to predict the oxidative capacity of humic quinones in dissolved organic matter: implication for pollutant degradation

Davide Palma[1] · Edith Parlanti[2] · Mahaut Sourzac[2] · Olivier Voldoire[3] · Aude Beauger[2] · Mohamad Sleiman[1] · Claire Richard[1]

Received: 15 June 2020 / Accepted: 6 November 2020 / Published online: 23 November 2020

Abstract

Dissolved organic matter (DOM) controls the degradation and sequestration of aquatic pollutants and, in turn, water quality. In particular, pollutant degradation is performed by oxidant species that are generated by exposure of DOM to solar light, yet, since DOM is a very complex mixture of poorly known substances, the relationships between potential oxidant precursors in DOM and their oxydative capacity is poorly known. Here, we hypothesized that production of oxidant species could be predicted using fluorescence analysis. We analysed water samples from an alluvial plain by fluorescence spectroscopy; the three-dimensional spectra were then decomposed into seven individual components using a multi-way algorithm. Components include a protein-like fluorophore, e.g. tryptophan-like and tyrosine-like, three humic fluorophores, 2-naphthoxyacetic acid, and a by-product. We compared component levels with the ability of water samples to generate reactive species under solar light. The results show a strong correlation between reactive species production and the intensity of two humic-like fluorophores assigned to reduced quinones. Monitoring these fluorophores should thus allow to predict the ability of DOM degradation of pollutants in surface waters.

Keywords Dissolved organic matter · Cut-off meander · Quinonic-like components · Triplet excited states · Singlet oxygen · Correlation

Introduction

Dissolved organic matter (DOM) encompasses ubiquitous natural components able to generate oxidant species under solar light exposure and thus to degrade aquatic pollutants in surface waters. Previous works have shown that the capacity of DOM to generate reactive species under solar irradiation could be predicted measuring its absorbance properties (Dalrymple et al 2010; Mckay et al. 2017; Peterson et al. 2012; Palma et al. 2020). Previous works also suggested that correlations may exist between DOM photoreactivity and fluorescence parameters (Coelho et al. 2011) or individual fluorescent components identified by deconvolution of the three-dimensional spectra by parallel factor analysis (PARAFAC, Timko et al. 2014; Bai et al. 2018; Batista et al. 2016).

Here, our goal was to investigate the fluorophores linked to the photochemical generation of oxidant species such as DOM triplet excited states (^{3}DOM*) and singlet oxygen (SO) on waters sampled in an experimental site. This site was chosen because it offers a variety of water types: riverine, underground and stagnant. The individual fluorescent components were identified using literature data and the OpenFluor database and their spatial and temporal distribution were determined. Finally, the exploration of correlations between component intensities and rates of oxidant species formation allowed to connect reactive species formation to

Electronic supplementary material The online version of this article (https://doi.org/10.1007/s10311-020-01137-z) contains supplementary material, which is available to authorized users.

✉ Claire Richard
Claire.richard@uca.fr

[1] Université Clermont Auvergne, CNRS, SIGMA-Clermont, ICCF, 63000 Clermont-Ferrand, France

[2] Université Bordeaux, CNRS, EPOC UMR 5805, 33405 Talence, France

[3] Université Clermont Auvergne, CNRS, GEOLAB, 63000 Clermont-Ferrand, France

the presence of reduced quinonic structures identified based on the literature data.

Experimental

Site description and samplings

The experimental site is the SOAHAL Observatory 'Système d'Observation d'une Annexe Hydraulique de l'ALlier' (Peiry et al 2014). This study area, previously described (Palma et al 2020), is a cut-off meander of the Allier River, a tributary of the Loire River situated in the temperate zone (Massif central, France). It includes the Auzon cut-off meander, the Allier River and its tributary Vendage, as well as two aquifers, the alluvial fluvial flow and the watershed ones (Figure SI-1). Water samples were collected in March, July and October 2018 in Allier River, in Vendage River, in the cut-off meander at sampling sites B4 and B7, and in the piezometers PZ1 and PZ5 (Figure SI-1).

Fluorescence spectra recording and deconvolution

The three-dimensional fluorescence spectra recording is described in Supporting Information. All fluorescence signals were normalized using the area under the Raman peak at excitation 350 nm of purified water; reverse osmosis RIOS 5 and Synergy-Millipore device, resistivity 18 MΩ cm, DOC < 0.1 mg L^{-1} (Cory and McKnight 2005). Solutions were diluted before measurement to have an absorbance < 0.1 at 250 nm, and the recorded spectra were multiplied by the dilution coefficient. Parallel factor analysis is classically used to decompose the three-dimensional spectra and facilitate the identification and quantification of independent underlying fluorescent signals, termed "components" (Murphy et al 2013). The multi-way parallel factor analysis model was run for 3 to 8 components with non-negativity constraints using the DOMFluor toolbox (ver. 1.7) for MATLAB (R14-6.5) as described by Stedmon and Bro (2008). Seven components were determined, based on the examination of the residuals from models, split half analysis and visual inspection of spectral shapes of each component, and compared to previously validated components using the OpenFluor fluorescence database (Murphy et al 2014).

Rates of reactive species production

2,4,6-Trimethylphenol (Sigma-Aldrich, certified reference material) was used to scavenge ^{3}DOM* while furfuryl alcohol (Sigma-Aldrich, 98%) to trap SO. The protocol used to measure the consumption of these probes and the processes used to establish the rate laws are described in SI and in Palma et al (2020). Briefly, the rate of 2,4,6-trimethylphenol consumption (R^{TMP}) is equal to

$$R^{TMP} = R^{3DOM*} \times \alpha_{TMP} = R_a \times \Phi_{3DOM*} \times \alpha_{TMP} \quad (1)$$

where R^{3DOM*} is the rate of ^{3}DOM* production and α_{TMP} the fraction of ^{3}DOM* trapped by 2,4,6-trimethylphenol. R_a is the rate of light absorption by DOM between 300 and 450 nm calculated using the Beer–Lambert law $I_a = I_0 \times (1 - 10^{-A})$, the absorption spectrum of DOM and the emission spectrum of the tubes, Φ_{3DOM*}, the quantum yield of ^{3}DOM* production. The rate of 2-hydroxypyranone formation (R^P), the main product of reaction between furfuryl alcohol and SO (chemical yield = 85%) is equal to:

$$R^P = 0.85 \times R^{SO} \times \alpha_{FFA} = 0.85 \times R_a \times \Phi_{SO} \times \alpha_{FFA} \quad (2)$$

where R^{SO} is the rate of SO production, Φ_{SO} is the quantum yield of SO production and α_{FFA} the fraction of SO trapped by furfuryl alcohol.

Statistical analyses

Statistical analyses were performed with the R statistical software (R version 3.6.1, R Foundation for Statistical Computing). To reveal the relationships between the DOM fluorescence characteristics and its capacity to generate reactive species under irradiation, principal component analysis was conducted on scaled and centred data of all samples and 10 variables, i.e. the 7 individual parallel factor analysis components, and the different rates. Pearson correlation coefficients were reported for all correlations where data were normally distributed. *P*-values < 0.01 were considered statistically significant.

Results and discussion

Assignment of the individual parallel factor analysis components

The contour plots of the 7 individual components determined by parallel factor analysis decomposition are presented in Fig. 1. Components C1 to C5 have been successfully matched in the OpenFluor database with similarity scores higher than 0.95. Component C1 (λ_{exc} = 300 and < 250) nm/λ_{em} = 390 nm) is a widespread component generally found in marine and terrestrial aquatic environments and attributed to low molecular weight substances (Osburn et al. 2011; Coble 2007). Component C2 (λ_{exc} = 280 nm/λ_{em} = 300, 340 nm) seems to gather the protein-like fluorophores with emission at 300 nm for tyrosine-like and the emission at 330–350 nm for tryptophane-like fluorophores (Coble 2007; Parlanti et al. 2000).

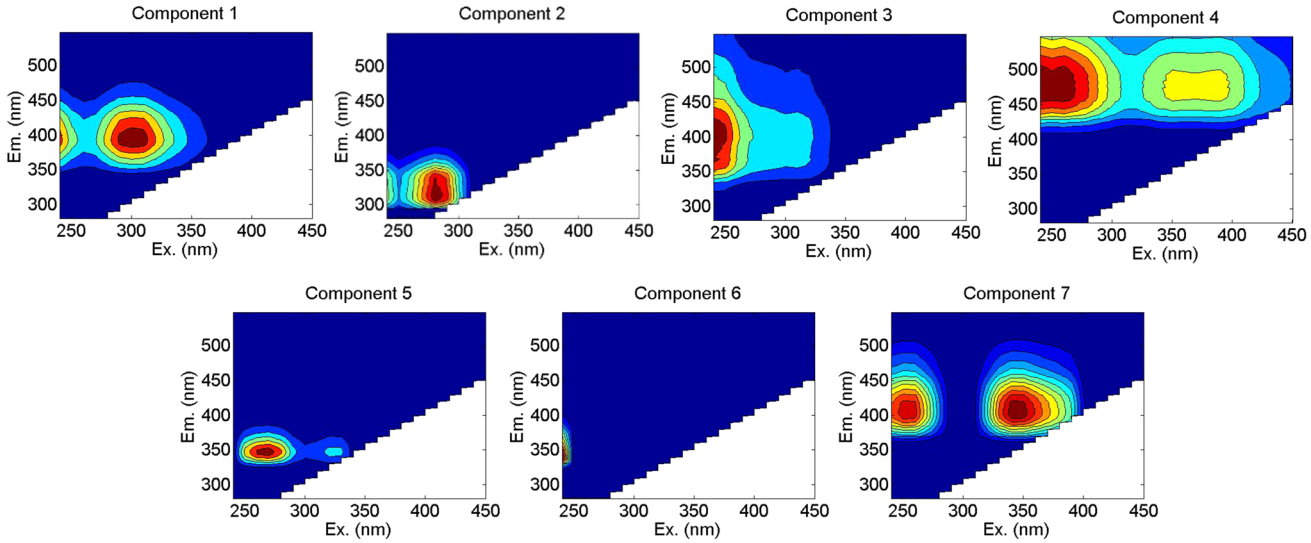

Fig. 1 Fluorescence signatures of the seven components identified by parallel factor analysis decomposition of the three-dimensional spectra. They were assigned by comparison with the literature or to commercial compound spectrum, to widespread low molecular weight component (Component 1—C1), to protein-like fluorophores (Component 2—C2), to (photo)degraded terrestrial component (Component 3—C3), to microbially reduced quinone-like fluorophores (Component 4—C4), to 2-naphthoxy-acetic acid (Component 5—C5), to a non-identified component probably linked to C5 (Component 6—C6), and to reduced quinone-like component (Component 7—C7)

Component C3 ($\lambda_{exc} = 245$ and 315 nm/$\lambda_{em} = 400$ nm) was already observed (Osburn et al 2012; Romero et al 2017; Stedmon et al 2003) and assigned as fluorophores from terrestrial origin possibly produced by (photo)degradation (Osburn et al 2012). Component C4 ($\lambda_{exc} = 260$ and 370 nm/$\lambda_{em} = 480$ nm) is also a widespread component that has been described as high molecular weight fluorophores (Kowalczuk et al 2013; Murphy et al 2006; Stedmon et al 2007). It was found to be produced during bacterial processing of DOM (Amaral et al 2016) and could derive from microbial metabolism (Romera-Castillo et al 2011).

Component C4 has also strong analogies with component SQ2 ($\lambda_{exc} = 270$ and 380 nm/$\lambda_{em} = 462$ nm) assigned by Cory and McKnight 2005 to reduced quinone-like component. Component C5 ($\lambda_{exc} = 270$ and 325 nm/$\lambda_{em} = 345$ nm) was assigned to 2-naphthoxy-acetic acid by comparison with an authentic sample (SI). 2-Naphthoxy-acetic acid is generally used for controlling of preharvest fruit drop on strawberries and tomatoes. The detection of this highly fluorescent anthropogenic compound in the cut-off meander water samples is explained by the presence of vegetable farming near the site.

Component C6 ($\lambda_{exc} < 245$ nm/$\lambda_{em} = 345$ nm) did not find matches in OpenFluor-database. At last, C7 had strong analogies with component labelled SQ3 ($\lambda_{exc} = 265$ and 345 nm/$\lambda_{em} = 412$ nm) assigned once again to a reduced quinone-like component (Cory and McKnight 2005).

Spatial and temporal distribution of the individual parallel factor analysis components

The spatial and temporal variations of the component fluorescence intensities are shown in Fig. 2. The intensity of 2-naphthoxy-acetic (C5) acid and C6 was particularly important in B4-July. Components C5 and C6 appeared together in Allier-July, B7-July, PZ5-July and Vendage-July suggesting that C6 could be a degradation product of 2-naphthoxy-acetic acid. C1 and C2 were detected in high amounts in PZ1-July, Allier River-July and B7-July, while in moderate amounts in Vendage River and Allier-River-October and in minor amounts in the other water samples. As a part of the cut-off meander was covered with aquatic plants in July, these results suggest a microbial or algal origin for C1 and C2. C3 was mainly present in Allier River and Vendage River, both characterized by the highest DOM aromaticity (Palma et al 2020). C4 and C7 were detected in all the samples in quite similar fluorescence intensities, suggesting that they could have common origins and fates. Higher intensities were found in July than in March or October and in River than in cut-off meander samples.

Correlation between individual parallel factor analysis components and photoreactivity of dissolved organic matter

Results on the dissolved organic matter (DOM) photoreactivity of the different samples are shown Fig. 3. The

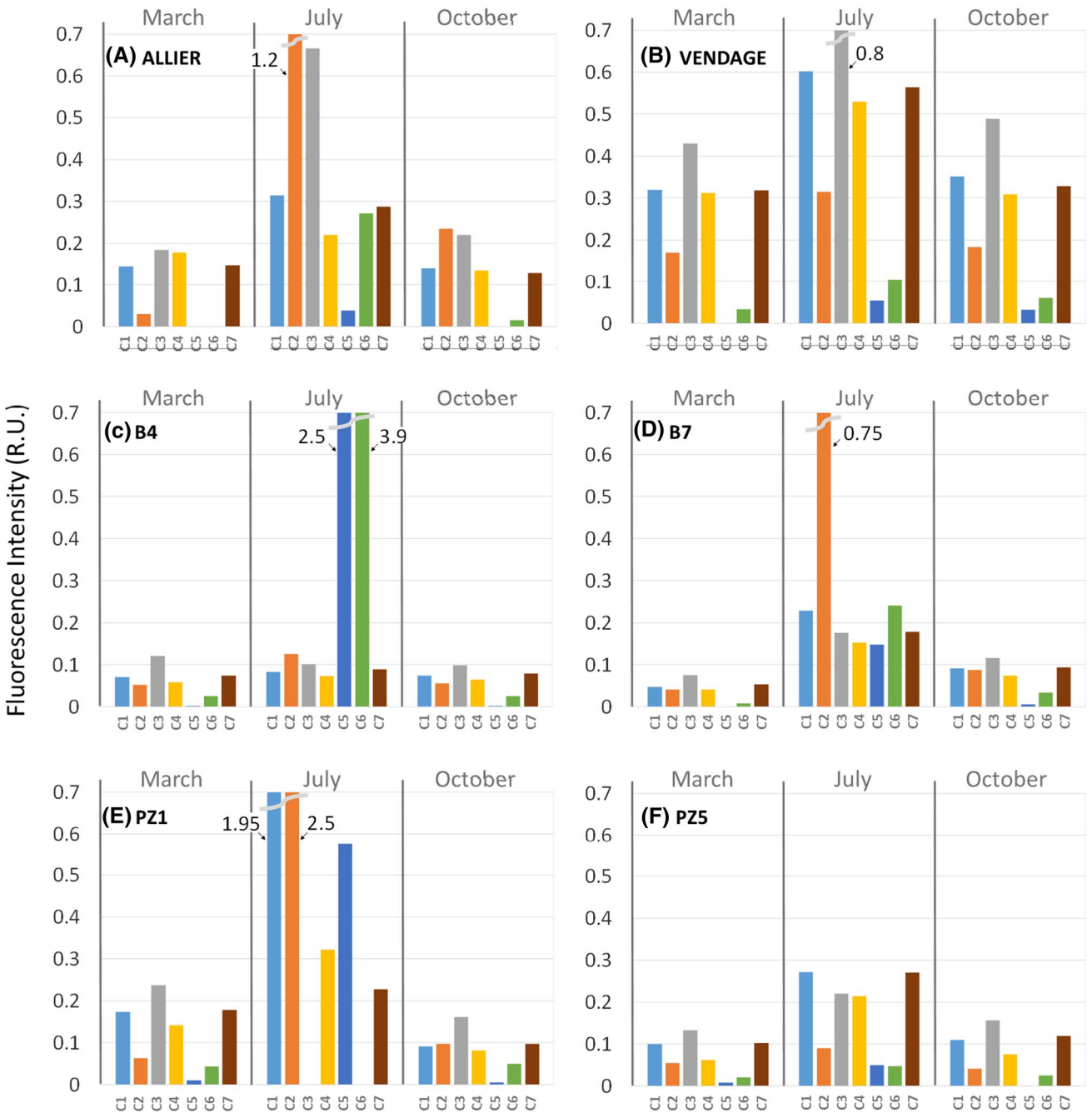

Fig. 2 Temporal variations of the seven components determined by parallel factor analysis decomposition—C1) widespread low molecular weight component; C2) protein-like fluorophores, C3) (photo)degraded terrestrial component; C4) microbially reduced quinone-like fluorophores, C5) 2-naphthoxy-acetic acid, C6) non-identified component probably linked to the component C5 and C7) reduced quinone-like component—for the six studied sites: **A** Allier, **B** Vendage, **C** cut-off meander sites B4, **D** cut-off meander sites B7, **E** piezometer PZ1 and **F** piezometer PZ5. Fluorescence intensities are reported in Raman units (R.U.)

rivers Allier and Vendage logically contained the more absorbing DOM (Fig. 3A) because their waters enrich in soil aromatic organic matter while crossing forests and fields areas. The rates of 2,4,6-trimethylphenol consumption (R^{TMP}, Fig. 3B) and the rates of hydroxypyranone formation (R^{P}, Fig. 3C) shows parallel variations with highest values in July and lowest values in B4 and B7 sampling sites.

As R^{TMP} was proportional to R^{3DOM*} Eq. (1) and R^{P} to R^{SO} Eq. (2) according to our mechanistic hypotheses, the

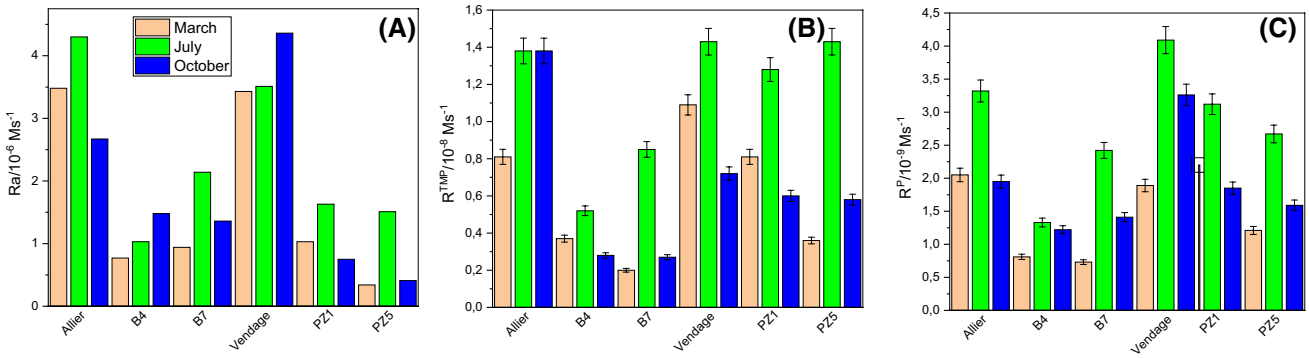

Fig. 3 Variations of dissolved organic matter (DOM) photoreactivity in the six studied sites: Allier, Vendage, cut-off meander sites B4, cut-off meander sites B7, PZ1 and PZ5, in March, July and October. **A** rate of light absorption (R_a), **B** rate of 2,4,6-trimethylphenol consumption (R^{TMP}), **C** rate of hydroxypyranone formation (R^P)

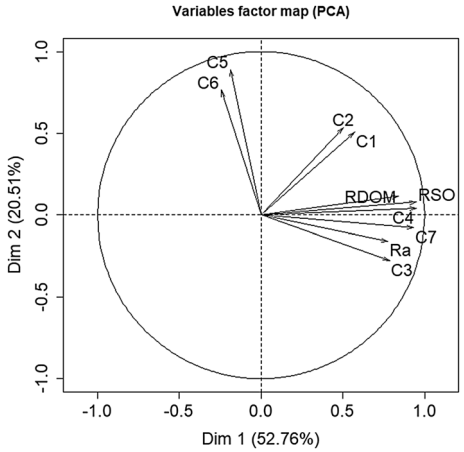

Fig. 4 Variable factor map from principal component analysis (PCA) obtained from 10 variables: the seven components determined by parallel factor analysis decomposition of the three-dimensional spectra (C1—widespread low molecular weight component, C2—protein-like fluorophores, C3—(photo)degraded terrestrial component, C4—microbially reduced quinone-like fluorophores, C5—2-naphthoxy-acetic acid, C6—non-identified component probably linked to the component C5 and C7—reduced quinone-like component, the rate of light absorption (R_a), the rate of triplet excited state formation (R^{3DOM*}) and the rate of singlet oxygen production (R^{SO})

principal component analysis of Fig. 4a is performed with R^{3DOM*} and R^{SO}. R^{3DOM*} and R^{SO} were positively correlated to each other ($R=0.8$, $p<0.01$) in accordance with the formation of singlet oxygen from ^{3}DOM*. Moreover, R^{3DOM*} was positively correlated to microbially derived fluorophores C4 and to reduced quinone-like component C7 ($R=0.74$ and 0.72, $p<0.01$, respectively), R^{SO} to C4, C7 and degraded terrestrial component C3 ($R=0.88$, 0.88 and 0.73, with $p<0.01$, respectively) and Ra to C3, C4 and C7 ($R=0.75$, 0.7 and 0.69, with $p<0.01$, respectively) (Fig. 4a and SI-4). The other components did not show any correlation. However, C1 assigned to low molecular weight substances was very near to protein-like fluorophores C2 on the variable factor map and C5, assigned to 2-naphthoxy-acetic acid, to non-identified component C6. It shows that C1 had common features with C2, and C5 with C6.

Previous works reported that the formation rate of singlet oxygen was coupled to the abundance of humic-like components emitting at long wavelength for DOM of both marine (Timko et al. 2014; Bai et al. 2018) and terrestrial origin (Batista et al. 2016; Coelho et al. 2011). Compared to these works, we were able to identify the moieties involved in the correlation, and we propose that C4 and C7 could be attributed to the reduced forms of quinonic humic-like components (Cory and McKnight 2005). This result is in line with the study of Zheng et al (2019) in which a positive correlation between electron accepting capacity of DOM, to which quinones strongly contribute, and the presence of one of the fluorescent parallel factor analysis components proposed to represent oxidized quinoid-like structures was reported.

Conclusion

We found a strong positive correlation between two individual parallel factor analysis components representing DOM quinonic moieties (C4 and C7) and DOM photoreactivity, specifically the generation of oxidant species like DOM triplet excited states and singlet oxygen. This finding confirms the role played by quinonic compounds in the sensitizing properties of natural organic matter and suggests that monitoring these compounds using fluorescence spectroscopy could be a valid approach for a rapid estimation of the sensitizing properties of DOM.

Acknowledgements This paper is part of a project that has received funding from the European Union's Horizon 2020 research and

innovation programme under the Marie Skłodowska-Curie Grant agreement No. 765860 (Aquality).

References

Amaral V, Graeber D, Calliari D, Alonso C (2016) Strong linkages between DOM optical properties and main clades of aquatic bacteria. Limnol Oceanogr 61:906–918. https://doi.org/10.1002/lno.10258

Bai Y, Cui Z, Su R (2018) Influence of DOM components, salinity, pH, nitrate, and bicarbonate on the indirect photodegradation of acetaminophen in simulated coastal waters. Chemosphere 205:108–117. https://doi.org/10.1016/j.chemosphere.2018.04.087

Batista APS, Teixeira ACSC, Cooper WJ, Cottrell BA (2016) Correlating the chemical and spectroscopic characteristics of natural organic matter with the photodegradation of sulfamerazine. Water Res 93:20–29. https://doi.org/10.1016/j.watres.2015.11.036

Coble PG (2007) Marine optical biogeochemistry: the chemistry of ocean color. Chem Rev 107:402–418. https://doi.org/10.1021/cr050350+

Coelho C, Guyot G, ter Halle A, Cavani L, Ciavatta C, Richard C (2011) Photoreactivity of humic substances: relationship between fluorescence and singlet oxygen production. Environ Chem Lett 9:447–451. https://doi.org/10.1007/s10311-010-0301-3

Cory RM, Mcknight DM (2005) Fluorescence spectroscopy reveals ubiquitous presence of oxidized and reduced quinones in DOM. Environ Sci Technol 39:8142–8149. https://doi.org/10.1021/es050696 2

Dalrymple RM, Carfagno AK, Sharpless CM (2010) Correlations between Dissolved Organic Matter Optical Properties and Quantum Yields of Singlet Oxygen and Hydrogen Peroxide. Environ Sci Technol 44(5824):5829. https://doi.org/10.1021/es101005u

Golanoski K, Fang S, Del Vecchio R, Blough NV (2012) Investigating the mechanism of phenol photooxidation by humic substances. Environ Sci Technol 46:3912–3920. https://doi.org/10.1021/es300142y

Kowalczuk P, Tilstone GH, Zabłocka M, Rottgers R, Thomas R (2013) Composition of dissolved organic matter along an atlantic meridional transect from fluorescence spectroscopy and parallel factor analysis. Mar Chem 157:170–184. https://doi.org/10.1016/j.marchem.2013.10.004

Mckay G, Huang W, Romera-Castillo C, Crouch JE, Rosario-Ortiz FL, Jaffé R (2017) Predicting reactive intermediate quantum yields from dissolved organic matter photolysis using optical properties and antioxidant capacity. Environ Sci Technol 51:5404–5413. https://doi.org/10.1021/acs.est.6b06372

Murphy KR, Ruiz G, Dunsmuir W, Waite T (2006) Optimized parameters for fluorescence-based verification of ballast water exchange by ships. Environ Sci Technol 40:2357–2362. https://doi.org/10.1021/es0519381

Murphy KR, Stedmon CA, Graeber D, Bro R (2013) Fluorescence spectroscopy and multi-way techniques. PARAFAC Anal Methods 5:6557–6566. https://doi.org/10.1039/c3ay41160e

Murphy KR, Stedmon CA, Wenig P, Bro R (2014) OpenFluor- an online spectral library of auto-fluorescence by organic compounds in the environment. Anal Methods 6:658–661. https://doi.org/10.1039/c3ay41935e

Osburn CL, Wigdahl CR, Fritz SC, Sarosb JE (2011) Dissolved organic matter composition and photoreactivity in prairie lakes of the U.S. Great Plains Limnol Oceanogr 56:2371–2390. https://doi.org/10.4319/lo.2011.56.6.2371

Osburn C, Osburn L, Handsel LT, Mikan MP, Paerl HW, Montgomery MT (2012) Fluorescence tracking of dissolved and particulate organic matter quality in a river-dominated estuary. Environ Sci Technol 46:8628–8636. https://doi.org/10.1021/es3007723l

Palma D, Sleiman M, Voldoire O, Beauger A, Parlanti E, Richard C (2020) Study of the dissolved organic matter (DOM) of the Auzon cut-off meander (Allier River, France) by spectral and photoreactivity approaches. Environ Sci Poll Res 27:26385–26394. https://doi.org/10.1007/s11356-020-09005-7

Parlanti E, Worz K, Geoffroy L, Lamotte M (2000) Dissolved organic matter fluorescence spectroscopy as a tool to estimate biological activity in a coastal zone submitted to anthropogenic inputs. Org Geochem 31:1765–1781. https://doi.org/10.1016/S0146-6380(00)00124-8

Peiry J-P, Beauger A, Celle-Jeanton H, Voldoire O, Casado A (2014) SOHAL: système d'observation d'une annexe hydraulique de l'Allier. Colloque de restitution du CPER Auvergne, Dec 2014, Clermont Ferrand, France

Peterson BM, McNally AM, Cory RM, Thoemke JD, Cotner JB, McNeill K (2012) Spatial and temporal distribution of singlet oxygen in lake superior. Environ Sci Technol 46:7222–7229. https://doi.org/10.1021/es301105e

Romera-Castillo CH, Sarmento XA, Alvarez-Salgado J, Gasol M, Marras C (2011) Net production and consumption of fluorescent colored dissolved organic matter by natural bacterial assemblages growing on marine phytoplankton exudates. Appl Environ Microbiol 77:7490–7498. https://doi.org/10.1128/AEM.00200-11

Romero CM, Engel RE, D'Andrilli J, Chen C, Zabinski C, Millera PR, Wallander R (2017) Bulk optical characterization of dissolved organic matter from semiarid wheat-based cropping systems. Geoderma 306:40–49. https://doi.org/10.1016/j.geoderma.2017.06.029

Sharpless CM (2012) Lifetimes of triplet dissolved natural organic matter (DOM) and the effect of $NaBH_4$ reduction on singlet oxygen quantum yields: Implications for DOM photophysics. Environ Sci Technol 46:4466–4473. https://doi.org/10.1021/es300217h

Stedmon CA, Markager S, Bro R (2003) Tracing DOM in aquatic environments using a new approach to fluorescence spectroscopy. Mar Chem 82:239–254. https://doi.org/10.1016/S0304-4203(03)00072-0

Stedmon CA, Thomas DN, Granskog M, Kaartokallio H, Papadimitriou S, Kuosa H (2007) Characteristics of dissolved organic matter in Baltic coastal sea ice: Allochthonous or autochthonous origins? Environ Sci Technol 41:7273–7279. https://doi.org/10.1021/es071210f

Stedmon CA, Bro R (2008) Characterizing dissolved organic matter fluorescence with parallel factor analysis: a tutorial. Limnol Oceanogr Meth 6:572–579. https://doi.org/10.4319/lom.2008.6.572

Timko SA, Romera-Castillo C, Jaff R, Cooper WJ (2014) Photo-reactivity of natural dissolved organic matter from fresh to marine waters in the Florida Everglades, USA. Environ Sci Process Impacts 16:866–878. https://doi.org/10.1039/C3EM00591G

Zheng X, Liu Y, Fu H, Qu X, Yan M, Zhang S, Zhu D (2019) Comparing electron donating/accepting capacities (EDC/EAC) between crop residue-derived dissolved black carbon and standard humic

substances. Sci Tot Environ 673:29–35. https://doi.org/10.1016/j.scitotenv.2019.04.022

Zhou H, Lian L, Yan S, Song W (2017) Insights into the photo-induced formation of reactive intermediates from effluent organic matter: The role of chemical constituents. Water Res 112:120–128. https://doi.org/10.1016/j.watres.2017.01.048